Magnetic Resonance Imaging–Based Three-Dimensional Bone Shape of the Knee Predicts Onset of Knee Osteoarthritis

Data From the Osteoarthritis Initiative

Tuhina Neogi,[1] Michael A. Bowes,[2] Jingbo Niu,[1] Kevin M. De Souza,[2] Graham R. Vincent,[2] Joyce Goggins,[1] Yuqing Zhang,[1] and David T. Felson[3]

Objective. To examine whether magnetic resonance imaging (MRI)–based 3-dimensional (3-D) bone shape predicts the onset of radiographic knee osteoarthritis (OA).

Methods. We conducted a case–control study using data from the Osteoarthritis Initiative by identifying knees that developed incident tibiofemoral radiographic knee OA (case knees) during followup, and matching them each to 2 random control knees. Using knee MRIs, we performed active appearance modeling of the femur, tibia, and patella and linear discriminant analysis to identify vectors that best classified knees with OA versus those without OA. Vectors were scaled such that −1 and +1 represented the mean non-OA and mean OA shapes, respectively. We examined the relation of 3-D bone shape to incident OA (new-onset Kellgren and Lawrence [K/L] grade ≥2) occurring 12 months later using conditional logistic regression.

Results. A total of 178 case knees (incident OA) were matched to 353 control knees. The whole joint (i.e., tibia, femur, and patella) 3-D bone shape vector had the strongest magnitude of effect, with knees in the highest tertile having a 3.0 times higher likelihood of developing incident radiographic knee OA 12 months later compared with those in the lowest tertile (95% confidence interval [95% CI] 1.8–5.0, $P < 0.0001$). The associations were even stronger among knees that had completely normal radiographs before incidence (K/L grade of 0) (odds ratio 12.5 [95% CI 4.0–39.3]). Bone shape at baseline, often several years before incidence, predicted later OA.

Conclusion. MRI-based 3-D bone shape predicted the later onset of radiographic OA. Further study is warranted to determine whether such methods can detect treatment effects in trials and provide insight into the pathophysiology of OA development.

[1]Tuhina Neogi, MD, PhD, FRCPC, Jingbo Niu, MD, DSc, Joyce Goggins, MPH, Yuqing Zhang, DSc: Boston University School of Medicine, Boston, Massachusetts; [2]Michael A. Bowes, PhD, Kevin M. De Souza, PhD, Graham R. Vincent, DPhil: Imorphics Ltd., Manchester, UK; [3]David T. Felson, MD, MPH: Boston University School of Medicine, Boston, Massachusetts, and University of Manchester, Manchester, UK.

Drs. Bowes, De Souza, and Vincent own stock or stock options in Imorphics Ltd.

Address correspondence to Tuhina Neogi, MD, PhD, FRCPC, Boston University School of Medicine, Clinical Epidemiology Research and Training Unit, 650 Albany Street, X Building, Suite 200, Boston, MA 02118. E-mail: tneogi@bu.edu.

Submitted for publication October 19, 2012; accepted in revised form April 18, 2013.

Knee osteoarthritis (OA) is a leading cause of disability among older adults in the US (1), with the burden rising in part due to aging of the population and increasing obesity (2). There are presently no therapies available to prevent OA or its progression. The current standard of using knee radiographs to identify OA onset or joint space width to monitor progression is likely not sensitive enough to accurately assess the effects of potentially promising treatments. For example, the risedronate (3) and oral inducible nitric oxide synthase inhibitor (4) trials did not meet their primary end points based on radiographic joint space narrowing despite supportive preliminary data, raising concerns about the

lack of sensitivity of radiography. Thus, there is a compelling need to develop improved imaging biomarkers for OA to enable the development and testing of treatments. Such imaging biomarkers would also help identify persons at risk of developing knee OA and/or rapid disease progression, permitting the study of pertinent risk factors and targeted enrollment into trials.

Because knee OA is thought to be a largely mechanically driven process (5), a promising target for an OA imaging biomarker may be to exploit the ability of bone to adapt to mechanical influences (6). In particular, bone can readily change its shape in response to stresses acting upon it (Wolff's law) (6,7), suggesting that such alterations may be feasibly assessed in a practical timeframe, making it attractive as a potential imaging end point for trials. Additionally, subtle differences in bone shape or geometry itself could lead to abnormal joint loading and predispose to OA.

Lending support to the importance of bone shape to OA, abnormalities such as congenital hip dysplasia and femoracetabular impingement, as well as more subtle femoracetabular shape differences identified through morphometric measurements or statistical modeling, have been associated with hip OA (8–11). Although the geometry of the knee may be more complex than that of the hip, differences in knee joint shape between ethnic groups have been identified (12). Tibiofemoral joint shape alterations on radiographs have been associated with prevalent knee OA cross-sectionally (13). However, some of the changes identified may have been related to position during image acquisition, and more generally, radiographs do not permit visualization of 3-dimensional (3-D) bone shape changes.

While magnetic resonance imaging (MRI) studies have described increased tibial plateau size and alterations of the bony surface contour (e.g., subchondral bone attrition) even during the preradiographic stage of OA (14–16), those findings do not fully capture the spectrum and complexity of the 3-D bone shape changes that occur in OA. More recently, a small cross-sectional study of 24 knees used MR images to evaluate the variability in knee articular surface geometry using statistical shape modeling to compare those with and those without OA (17).

With the increased availability and use of MRI, 3-D bone shape changes related to knee OA can now be more readily characterized on a larger scale using more advanced statistical modeling methods to detect subtle shape variations for improved sensitivity. Using data from the Osteoarthritis Initiative (OAI), we examined the ability of 3-D bone shape to predict the incidence of knee OA at least 12 months prior to its onset.

PATIENTS AND METHODS

Study sample. We used publicly available data from the OAI, which is a longitudinal observational cohort study with the objective of investigating the natural history of and risk factors for knee OA. Subjects ages 45–79 who had or were at high risk of knee OA were recruited from 4 clinical centers across the US. Details of the cohort have been published elsewhere (18) and can be found on the OAI website at http://oai.epi-ucsf.org/datarelease/StudyOverview.asp.

Imaging. *Knee radiography.* Bilateral posteroanterior, fixed-flexion, weight-bearing knee radiographs were obtained at baseline and annually (19). In this study, we used the centrally adjudicated radiographic reading data from baseline to the 48-month clinic visit, inclusively. Radiographs were read by an academically based radiologist and 2 rheumatologists in a panel of 3, with disagreement resolved by adjudication (20). Incident tibiofemoral radiographic knee OA was defined as a new-onset Kellgren and Lawrence (K/L) grade of ≥ 2 identified in a followup study visit (i.e., at 12, 24, 36, or 48 months) among knees that had a K/L grade of <2 at baseline. As per the OAI central readings, new-onset osteophytes with no narrowing were not considered to indicate incident OA (21). Incident knee OA could include incident medial or lateral tibiofemoral OA.

Magnetic resonance imaging. Participants underwent bilateral knee MRI (using a Siemens Trio 3.0T scanner) at baseline and annually. We used the sagittal 3-D double-echo steady-state with water excitation sequence for determination of the 3-D bone shape.

Statistical modeling of 3-D bone shape. Below we outline the 2 independent training sets used to develop the model employed in our analyses of a third independent test set.

We used an independent training set of 96 knees to train models used in automatic segmentation, utilizing active appearance models (AAMs). AAMs are a form of statistical shape modeling method that learns the variation in shape and gray-scale texture ("appearance") of objects from a training set (such as the bones from an MRI), and encodes shape and appearance as principal components (22,23). AAMs for the femur, tibia, and patella were built using custom software based on published AAM methodology (22) (Imorphics) from 96 examples chosen so as to contain approximately equal numbers of knees with each K/L grade. All models within this study were generated in order to account for 98% of the variance in the shape data from the training set. During the model building process, principal components are added until this number is reached. This resulted in 69 principal components for the femur shape, 66 for the tibia, and 59 for the patella. Once trained, AAMs can automatically segment bones in MR images by matching principal components of shape and appearance using the least squares sum of residuals. As a consequence of this process, each time a new image is searched, the distance along each of the principal components for the object is recorded. This has the effect of reducing shape dimensionality; in the case of the femur, this reduces a triangulated mesh of >100,000 points to 69 floating point
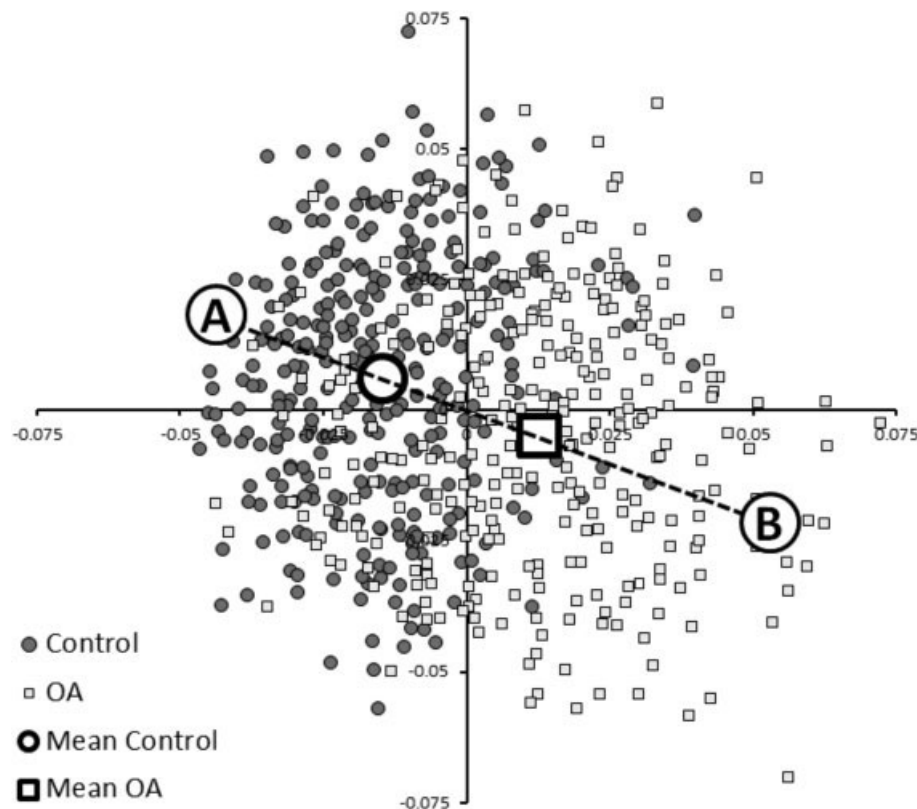
Figure 1. Sammon plots illustrating the shape distributions of the 607 femurs used in the training set. Linear discriminant analysis was used to determine the best single vector that discriminated the 2 groups (e.g., nonosteoarthritic [non-OA; A] versus OA [B]). The results for each individual femur are encoded as 70 principal components, creating a 70-dimensional value. The Sammon plot reduces these 70 dimensions into 2 dimensions while preserving the distances between shapes as far as possible. The labels "A" and "B" represent shapes at the 95% confidence boundary of a line drawn between the mean non-OA (control) and mean OA shapes.

values, one for each principal component in the model. The accuracy of the segmentations for the knee has been validated previously (24,25).

For our particular models, the accuracy of the automated segmentations was further assessed using test–retest MRIs for 19 participants (38 images) with no OA to moderate degrees of clinical OA, prepared as a pilot study for OAI, using the same MRI sequence (26). The bone surface was manually segmented as previously described (27). Mean point-to-surface distances were calculated between the manual and automated segmentations. Mean point-to-surface errors were as follows: for the femur, 0.49 mm; for the tibia, 0.53 mm; and for the patella, 0.57 mm (i.e., each approximately the size of 1 voxel).

We used a second independent training set to identify vectors within this shape space that could discriminate between distinct groups (e.g., OA and non-OA) using linear discriminant analysis (LDA), a form of supervised learning (28,29). LDA is used in pattern recognition and machine learning to find features that differentiate objects into separate groups (30), such as in medical imaging (e.g., neuroimaging) and facial recognition (31,32). LDA identifies the line in multidimensional space that best separates 2 groups. This further reduces the shape dimensionality to a single scalar value, which

is the distance along the LDA vector for each bone or combination of bones. We used a total of 607 knees (1 knee per person) from the OAI (296 with a K/L grade of 0 or 1 and 311 with a K/L grade of 2–4; median K/L grade of 3) (independent of the training set used to develop the AAM) to train the LDA vectors. The 607 images were searched using these AAMs, and the values for the principal components were recorded for each of the femur, tibia, and patella bones. The point sets of the femur and tibia were combined, and a shape model was built for the combined femur and tibia shape. A combined model of femur, tibia, and patella was also constructed. LDA was performed with the principal components for each bone as inputs, with each example labeled as OA or non-OA. The distribution of the femur shapes in the training set is shown in Figure 1 using a Sammon plot, a nonlinear dimension reduction that displays the 607 results in 2 dimensions while preserving the distances between examples as far as possible (33).

New bone shapes (e.g., those generated by an AAM search of the case–control study sample for this study) can be expressed as principal components, which in turn are projected onto the LDA vector. The distance along the vector is then recorded. Distance along the vector was normalized by setting

the mean non-OA shape to −1 and the mean OA shape to +1. Reproducibility of the method was tested in a separate set of 35 OA knees that were imaged 1 week apart, using the same OAI image acquisition sequence at a single OAI site (27). Reproducibility of the method was good, with the smallest detectable difference (95% confidence limits on a Bland-Altman plot) being 0.3 normalized units for the whole-joint model.

Visualization of changes in the population shape. Extreme examples of OA and non-OA shapes were created by finding the points at −3SD of the OA group and +3SD of the non-OA group, on a line passing through the means of the OA and non-OA groups (Figure 1). These were examined using a 3-D viewer (Imorphics).

Statistical analysis. We conducted a matched case–control study. Each knee that was identified as having developed incident tibiofemoral radiographic knee OA (case) was matched for baseline K/L grade to 2 randomly selected control knees that remained free of tibiofemoral OA at the same clinic visit as when incident OA was identified in the case knee (the index visit). We labeled this incident knee OA even though the absence of radiographic image assessment of the patellofemoral joint prohibited our evaluation of incidence there. We included in our study sample all knees that developed incident knee OA at any time during followup as well as their matched control knees. For individuals in whom both knees could be selected for this study, we randomly selected a single knee (n = 25).

We evaluated the following 5 3-D bone shape vectors as predictors of incidence: each bone separately (femur, tibia, and patella), femur and tibia together (tibiofemoral), and whole joint (femur, tibia, and patella combined). We first examined the relationship of the 3-D whole-bone shape vectors 12 months prior to the index visit to the risk of incident radiographic knee OA (i.e., occurring 12 months later) using conditional logistic regression. That is, we used 3-D bone shape data from the clinic visit 12 months prior to the occurrence of incident radiographic knee OA (or the index visit for the control knees). We repeated these analyses using only those case and control knees that had a K/L grade of 0 at baseline to reduce the likelihood that changes of early OA (at a K/L grade of 1) were reflected in the 3-D bone shape. We also examined the relationship of 3-D bone shape at the baseline OAI study visit (i.e., irrespective of time of later incident disease) to the occurrence of incident radiographic knee OA at any time during followup OAI visits. Finally, we evaluated the relationship of 3-D bone shape to incident radiographic knee OA occurring concurrently (i.e., 3-D bone shape vector from the same visit at which incident radiographic knee OA occurred) to confirm our prior findings that bone shape was related to concurrent OA (34).

The 3-D bone shape vectors were assessed as continuous variables as well as categorized into tertiles, with the highest tertile containing values closer to the mean OA shape, while the lowest tertile contained values closer to the mean

Table 1. Characteristics of the cases and controls*

	Cases (n = 178)	Controls (n = 353)	P
Age, years	61.3 ± 8.5	61.2 ± 9.1	0.8
BMI	29.4 ± 4.5	28.2 ± 4.5	0.004
No. (%) women	110 (61.8)	223 (63.2)	0.8
No. (%) white	150 (84.3)	312 (88.3)	0.2
No. (%) with a K/L grade of 0	46 (25.8)	92 (26.1)	1.0
No. (%) with a K/L grade of 1	132 (74.2)	261 (73.9)	
3-D bone shape vectors			
Whole joint (femur, tibia, patella)			
Baseline	−0.32 ± 0.50	−0.52 ± 0.53	<0.0001
12 months prior to incident OA	−0.23 ± 0.52	−0.51 ± 0.54	<0.0001
At incident OA	−0.01 ± 0.53	−0.44 ± 0.57	<0.0001
Tibiofemoral joint (femur, tibia)			
Baseline	−0.36 ± 0.55	−0.54 ± 0.54	0.0002
12 months prior to incident OA	−0.27 ± 0.56	−0.52 ± 0.57	<0.0001
At incident OA	−0.04 ± 0.55	−0.46 ± 0.59	<0.0001
Femur only			
Baseline	−0.42 ± 0.62	−0.63 ± 0.65	0.0001
12 months prior to incident OA	−0.33 ± 0.62	−0.63 ± 0.67	<0.0001
At incident OA	−0.10 ± 0.61	−0.56 ± 0.70	<0.0001
Tibia only			
Baseline	−0.40 ± 0.74	−0.50 ± 0.69	0.1
12 months prior to incident OA	−0.28 ± 0.78	−0.47 ± 0.72	0.005
At incident OA	−0.04 ± 0.76	−0.40 ± 0.74	<0.0001
Patella only			
Baseline	−0.25 ± 0.96	−0.51 ± 0.97	0.003
12 months prior to incident OA	−0.10 ± 1.00	−0.46 ± 0.96	<0.0001
At incident OA	+0.15 ± 1.06	−0.37 ± 1.05	<0.0001

* Except where indicated otherwise, values are the mean ± SD. BMI = body mass index; K/L = Kellgren and Lawrence; 3-D = 3-dimensional; OA = osteoarthritis.

Table 2. Relationship of 5 3-D bone shape vectors 12 months prior to the index visit to risk of incident radiographic knee OA*

3-D bone shape vector	% of case knees with incident radiographic knee OA	Crude OR	Adjusted OR (95% CI)†	P‡
Whole joint (femur, tibia, and patella)				
Highest tertile	47	3.3	3.0 (1.8–5.0)	<0.0001
Middle tertile	31	1.6	1.5 (0.9–2.5)	
Lowest tertile (reference)	22	1.0	1.0	
Per SD unit change toward mean OA shape	–	1.7	1.7 (1.4–2.1)	<0.0001
Tibiofemoral joint (femur and tibia)				
Highest tertile	43	2.8	2.5 (1.5–4.2)	0.0004
Middle tertile	35	2.0	1.9 (1.1–3.1)	
Lowest tertile (reference)	22	1.0	1.0	
Per SD unit change toward mean OA shape	–	1.6	1.5 (1.2–1.9)	<0.0001
Femur only				
Highest tertile	44	3.0	2.7 (1.7–4.5)	<0.0001
Middle tertile	36	2.1	2.0 (1.2–3.3)	
Lowest tertile (reference)	21	1.0	1.0	
Per SD unit change toward mean OA shape	–	1.6	1.5 (1.3–1.9)	0.0001
Tibia only				
Highest tertile	39	1.6	1.5 (0.9–2.4)	0.08
Middle tertile	32	1.1	1.1 (0.7–1.8)	
Lowest tertile (reference)	29	1.0	1.0	
Per SD unit change toward mean OA shape	–	1.3	1.3 (1.1–1.5)	0.01
Patella only				
Highest tertile	47	2.4	2.2 (1.3–3.4)	0.0009
Middle tertile	27	1.0	0.9 (0.6–1.4)	
Lowest tertile (reference)	27	1.0	1.0	
Per SD unit change toward mean OA shape	–	1.5	1.4 (1.2–1.7)	0.0005

* The vector range for the 3-dimensional (3-D) bone shape is −1 (mean nonosteoarthritic [non-OA] shape) to +1 (mean OA shape); therefore, the lowest tertile is the reference group. OR = odds ratio; 95% CI = 95% confidence interval.
† Adjusted for age, sex, and body mass index.
‡ P values for the tertiles are P for linear trend.

non-OA shape. Analyses were adjusted for age, sex, and body mass index (BMI).

RESULTS

Among knees without radiographic OA at baseline in the OAI, incident radiographic OA developed in 178 knees during the followup period. These were matched to 353 control knees. As can be seen in Table 1, the average age of the cases and controls was 61 years, the majority were female and white, and, as expected, the BMI was slightly higher in cases than controls.

The mean 3-D bone shape vectors increased (i.e., became more "OA-like") from baseline to the visit 12 months prior to the identification of incident radiographic knee OA to the visit at which incident radiographic knee OA was identified among case knees, while the 3-D bone shape vectors remained stable for the control knees over these 3 time points (Table 1). For example, for the whole-joint 3-D bone shape vector, which incorporated the femur, tibia, and patella, the mean values for the case knees were −0.32 at baseline, −0.23 at the visit 12 months prior to the identification of incident radiographic knee OA, and −0.01 at the visit when incident radiographic knee OA was identified, whereas the corresponding values were −0.52, −0.51, and −0.44 for the control knees.

Each of the 5 3-D bone shape vectors 12 months prior to the index visit was significantly associated with incident radiographic knee OA (Table 2). The 3-D bone shape vector that included the whole joint (i.e., all 3 bones) had the strongest magnitude of effect, with those knees in the highest tertile having a 3 times higher likelihood of developing incident radiographic knee OA 12 months later compared with those in the lowest tertile (95% confidence interval [95% CI] 1.8–5.0; $P < 0.0001$). There was also a dose-response relationship between the whole-joint 3-D bone shape vector and risk of incident radiographic knee OA ($P < 0.0001$) when assessed as tertiles as well as a continuous vector. Each SD unit change toward the mean OA shape was associated with a 68% higher risk of incident radiographic knee OA (95% CI 1.4–2.1, $P < 0.0001$) (Table 2). The 3-D bone shape vector of the femur alone had the largest effect among each of the individual bone vectors, with those in

Table 3. Relationship of 5 3-D bone shape vectors to risk of incident radiographic knee OA among knees that had a K/L score of 0 at baseline and in the whole sample concurrently at the time of incident OA*

3-D bone shape vector	Relationship of 3-D bone shape 12 months prior to incident radiographic knee OA among knees that had a K/L grade of 0 at baseline		Relationship of 3-D bone shape concurrently with incident radiographic knee OA	
	Adjusted OR (95% CI)†	P‡	Adjusted OR (95% CI)†	P‡
Whole joint (femur, tibia, and patella)				
Highest tertile	12.5 (4.0–39.3)	<0.0001	9.6 (5.3–17.5)	<0.0001
Middle tertile	1.7 (0.6–5.2)		4.2 (2.4–7.6)	
Lowest tertile (reference)	1.0		1.0	
Per SD unit change toward mean OA shape	2.9 (1.7–4.7)	<0.0001	2.3 (1.8–2.9)	<0.0001
Tibiofemoral joint (femur and tibia)				
Highest tertile	7.1 (2.5–20.1)	0.0002	6.4 (3.7–11.2)	<0.0001
Middle tertile	3.6 (1.3–9.6)		3.0 (1.7–5.3)	
Lowest tertile (reference)	1.0		1.0	
Per SD unit change toward mean OA shape	2.2 (1.4–3.5)	0.0007	2.1 (1.7–2.7)	<0.0001
Femur only				
Highest tertile	6.5 (2.3–18.3)	0.0003	6.5 (3.7–11.3)	<0.0001
Middle tertile	4.1 (1.5–11.1)		3.8 (2.2–6.5)	
Lowest tertile (reference)	1.0		1.0	
Per SD unit change toward mean OA shape	2.2 (1.4–3.5)	0.0008	2.1 (1.7–2.6)	<0.0001
Tibia only				
Highest tertile	3.7 (1.4–9.7)	0.007	2.9 (1.8–4.7)	<0.0001
Middle tertile	3.5 (1.3–8.9)		1.7 (1.1–2.8)	
Lowest tertile (reference)	1.0		1.0	
Per SD unit change toward mean OA shape	1.7 (1.1–2.6)	0.01	1.6 (1.5–2.0)	<0.0001
Patella only				
Highest tertile	2.7 (1.0–7.1)	0.05	3.3 (2.0–5.4)	<0.0001
Middle tertile	1.0 (0.4–2.7)		1.8 (1.1–3.0)	
Lowest tertile (reference)	1.0		1.0	
Per SD unit change toward mean OA shape	1.8 (1.1–2.7)	0.01	1.6 (1.3–2.0)	<0.0001

* The vector range for the 3-dimensional (3-D) bone shape is −1 (mean nonosteoarthritic [non-OA] shape) to +1 (mean OA shape); therefore, the lowest tertile is the reference group. K/L = Kellgren and Lawrence; OR = odds ratio; 95% CI = 95% confidence interval.
† Adjusted for age, sex, and body mass index.
‡ P values for the tertiles are P for linear trend.

the highest tertile having a 2.7 times higher chance than those in the lowest tertile of developing incident radiographic knee OA 12 months later (95% CI 1.7–4.5, $P <$ 0.0001). Of note, adjustment for the important potential confounders did not appreciably alter the effect estimates from the crude estimates, suggesting that the associations noted were not substantially influenced by age, sex, or BMI (Table 2).

Because knees with a K/L grade of 1 may have early changes of OA that could be reflected in the 3-D bone shape, we repeated the above analyses limited to those knees that had a K/L grade of 0 at baseline (n = 46). These knees were matched to 92 randomly selected control knees that also had a K/L grade of 0 at baseline. In these analyses, despite smaller numbers limiting precision, strong relationships were noted (Table 3). For example, knees in the highest tertile of the whole-joint vector 12 months prior to the index visit were 12.5 times

more likely to develop incident radiographic knee OA than knees in the lowest tertile (95% CI 4.0–39.3, $P <$ 0.0001). Again, the femur 3-D bone shape vector performed the best of the 3 individual bone vectors (OR 6.5 for highest versus lowest tertile [95% CI 2.3–18.3], $P =$ 0.0004). All 3-D bone shape vectors were significantly associated with incident radiographic knee OA among these knees with a K/L grade of 0 at baseline.

Because the onset of knee OA can occur at any time after a baseline study visit, we assessed the ability of 3-D bone shape from the baseline visit to predict the later occurrence of incident knee OA, irrespective of the timing of OA onset. In these analyses, the median time from the baseline OAI visit to the study visit at which incident OA was identified was 24 months. As can be seen in Table 4 (first results column), the magnitudes of effect were similar to those obtained with 3-D bone shape 12 months prior to the onset of radiographic knee

Table 4. Relationship of 5 baseline 3-D bone shape vectors to risk of incident radiographic knee OA in the whole sample and among knees that had a K/L score of 0 at baseline*

3-D bone shape vector	Relationship of baseline 3-D bone shape to incident radiographic OA in the whole sample				Relationship of baseline 3-D bone shape to incident radiographic OA among knees that had a K/L grade of 0 at baseline			
	Incident radiographic knee OA, irrespective of time of OA onset		Incident radiographic knee OA, occurring 24–48 months later		Incident radiographic knee OA, irrespective of time of OA onset		Incident radiographic knee OA, occurring 24–48 months later	
	Adjusted OR (95% CI)†	P‡	Adjusted OR (95% CI)†	P‡	Adjusted OR (95% CI)†	P‡	Adjusted OR (95% CI)†	P‡
Whole joint (femur, tibia, and patella)								
Highest tertile	2.5 (1.5–4.1)	0.0005	3.0 (1.5–6.0)	0.003	6.2 (2.1–18.4)	0.001	6.6 (1.8–24.9)	0.005
Middle tertile	1.8 (1.1–2.9)		2.6 (1.3–5.1)		2.0 (0.8–5.4)		2.2 (0.7–7.0)	
Lowest tertile (reference)	1.0		1.0		1.0		1.0	
Per SD unit change toward mean OA shape	1.5 (1.2–1.8)	0.0003	1.6 (1.2–2.1)	0.001	2.0 (1.3–3.1)	0.0009	2.5 (1.4–4.6)	0.002
Tibiofemoral joint (femur and tibia)								
Highest tertile	1.8 (1.1–2.9)	0.03	2.4 (1.2–4.7)	0.01	4.2 (1.4–12.3)	0.008	6.0 (1.6–22.3)	0.006
Middle tertile	1.6 (1.0–2.6)		2.3 (1.2–4.5)		2.8 (1.0–7.3)		3.1 (1.0–9.6)	
Lowest tertile (reference)	1.0		1.0		1.0		1.0	
Per SD unit change toward mean OA shape	1.3 (1.1–1.6)	0.003	1.5 (1.2–2.0)	0.002	1.7 (1.2–2.5)	0.004	2.4 (1.4–4.1)	0.002
Femur only								
Highest tertile	2.0 (1.2–3.3)	0.006	3.5 (1.7–6.9)	0.0004	3.9 (1.4–10.5)	0.009	4.8 (1.5–15.6)	0.006
Middle tertile	1.8 (1.1–2.9)		2.8 (1.4–5.5)		1.8 (0.7–4.7)		1.5 (0.5–4.8)	
Lowest tertile (reference)	1.0		1.0		1.0		1.0	
Per SD unit change toward mean OA shape	1.4 (1.1–1.7)	0.002	1.7 (1.3–2.3)	0.0002	1.6 (1.1–2.3)	0.007	2.2 (1.3–5.5)	0.002
Tibia only								
Highest tertile	1.2 (0.8–1.9)	0.4	1.4 (0.7–2.6)	0.3	2.6 (1.0–7.0)	0.04	2.3 (0.7–7.2)	0.1
Middle tertile	1.0 (0.6–1.6)		1.3 (0.7–2.4)		1.0 (0.8–4.7)		1.9 (0.7–5.3)	
Lowest tertile (reference)	1.0		1.0		1.0		1.0	
Per SD unit change toward mean OA shape	1.1 (0.9–1.4)	0.2	1.2 (0.9–1.5)	0.2	1.5 (1.0–2.3)	0.06	1.5 (0.9–2.4)	0.1
Patella only								
Highest tertile	1.9 (1.1–3.0)	0.01	1.6 (0.8–3.2)	0.2	3.0 (1.1–8.3)	0.04	3.7 (1.0–14.0)	0.06
Middle tertile	1.4 (0.9–2.3)		1.5 (0.8–2.8)		1.7 (0.7–4.2)		1.3 (0.4–4.0)	
Lowest tertile (reference)	1.0		1.0		1.0		1.0	
Per SD unit change toward mean OA shape	1.3 (1.1–1.6)	0.01	1.2 (0.9–1.6)	0.1	1.5 (1.0–2.2)	0.07	1.5 (0.9–2.7)	0.1

* The vector range for the 3-dimensional (3-D) bone shape is −1 (mean nonosteoarthritic [non-OA] shape) to +1 (mean OA shape); therefore, the lowest tertile is the reference group. K/L = Kellgren and Lawrence; OR = odds ratio; 95% CI = 95% confidence interval.
† Adjusted for age, sex, and body mass index.
‡ P values for the tertiles are P for linear trend.

OA (Table 2), suggesting that the vector can robustly discriminate knees that will develop OA in the future (i.e., 12, 24, 36, or 48 months later) from those that will not. That is, once a certain shape is present (i.e., at baseline), there is a high likelihood of developing OA at some point in the future, even years later.

When we further excluded the case knees that developed incident OA at 12 months (n = 82) (and their matched controls) to ensure that this group did not unduly influence these results, the magnitudes of effect remained similar. For example, for the knees in the highest tertile of the whole-joint vector, the OR was 3.0

(95% CI 1.5–6.0, P = 0.002) when knees with incident OA at 12 months were excluded, compared with an OR of 2.5 (95% CI 1.5–4.1, P = 0.0004) for the whole sample (Table 4, second results column compared with first results column). Larger effect estimates were also noted for knees that had a K/L grade of 0 at baseline in terms of predicting OA onset at any one of the later time points, as well as when knees with incident OA at 12 months were excluded (e.g., whole-joint vector OR 6.2 [P = 0.001] and OR 6.6 [P = 0.005] for highest versus lowest tertile for onset at any time point and for exclusion of onset at 12 months, respectively) (Table 4,
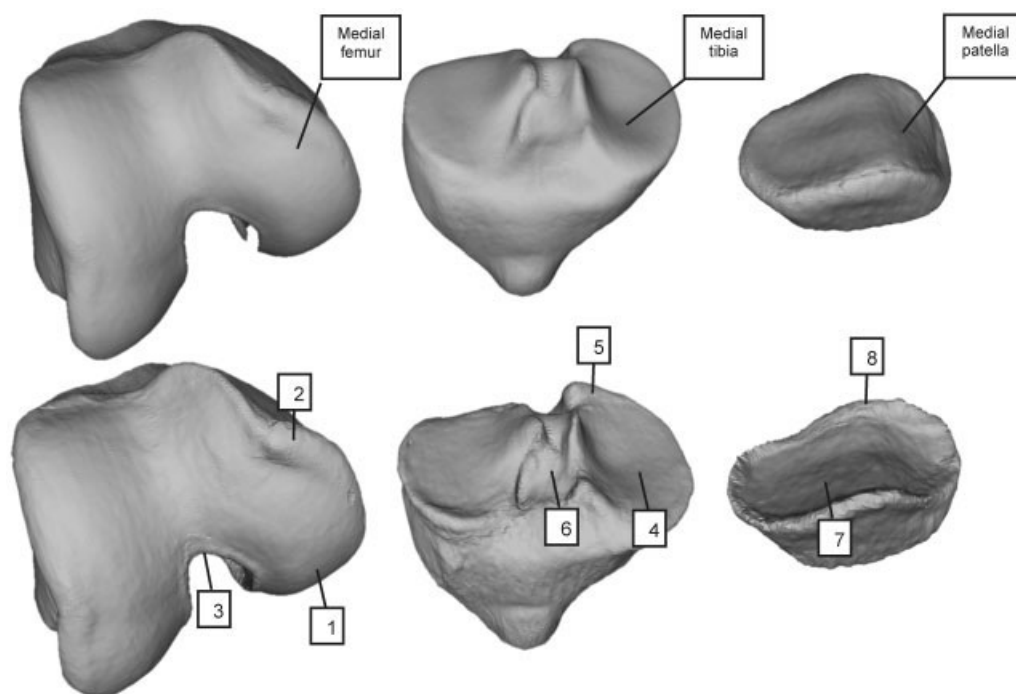
Figure 2. Three-dimensional visualization of osteoarthritis (OA) and control shapes. Top, Control shapes for the femur, tibia, and patella. Bottom, OA shapes for the femur, tibia, and patella. With OA, the femur shape changes include a widening and flattening of the condyles (**1**), an increased ridge of osteophytic growth around the cartilage plate (**2**), and narrowing of the notch (**3**). Tibia shape changes include a widening and flattening of the condyles (**4**), an increased ridge of osteophytic growth around the cartilage plate (**5**), and tibial spines moving closer together (**6**). The patella demonstrates similar patterns of increased cartilage plate size (**7**) and osteophytic ridge (**8**).

third and fourth results columns). This indicates that 3-D bone shape from the baseline visit could discriminate which groups of knees were highly likely to develop OA 24–48 months later, even among knees with a K/L grade of 0 at baseline (Table 4, second and fourth results columns).

When we examined bone shape at the same study visit as that of OA incidence, the relationship between bone shape and OA was strong, confirming prior findings (Table 3) (34). Similar to the findings described above, the whole-joint 3-D bone shape vector had the strongest relationship to incident radiographic knee OA, and the femur had the strongest relationship among each of the individual bones.

Figure 2 depicts examples of the OA and non-OA shapes for the population within the LDA training set represented by "A" and "B" in Figure 1. Differences in femur shape between OA and non-OA shapes include a general widening and flattening of the condyles on the medial side, and an increased ridge of "osteophytic" growth around all of the cartilage plate, along with a narrowing of the notch, in the OA sample. Differences

in tibial shape include a corresponding widening and flattening of the condyles, and an increased ridge of "osteophytic" growth around all of the cartilage plates, with the tibial spines moving closer together. The patella also has an increased cartilage plate size accompanied by an osteophytic ridge.

DISCUSSION

This is the first large-scale study of 3-D shape vectors to identify an imaging-based biomarker in knees without radiographic tibiofemoral OA at baseline. This also represents the first effort to examine whole-joint bone shape (comprising 3-D bone shapes of the femur, tibia, and patella) as a predictor of subsequent disease development. Importantly, this study is not only the first to demonstrate the properties of a statistical shape model containing OA examples, but also confirms that the measures are useful with an independent test set. We have demonstrated that 3-D vectors, trained on OA and non-OA shapes, can identify knees without OA that are at risk of developing OA 12 months later and beyond,

and that the position along this vector is associated with OA incidence.

That bone can change dynamically to such an extent that it is measurable during the course of disease is not surprising. Subchondral bone in OA has increased thickness and volume, leading to alterations in apparent and material bone density (35–39). Alterations in trabecular bone structure in knee OA have also been identified (40–43). In the high bone turnover state of OA, which can be detected by scintigraphy (44), mineral deposition may be attenuated, leading to relative hypomineralization and weaker bone that is more easily deformed (38,45). Other well-known changes in bone shape in knee OA include osteophyte formation and growth, hallmarks of OA, increased tibial plateau size, and alterations of the bony surface contour (subchondral bone attrition) (14–16). Changes in the intercondylar notch have also been noted previously (46,47), but the whole 3-D shape has not been described before, nor has the relative scale of the change. Our work confirms and extends these previous observations.

Importantly, the normal functioning of diarthrodial joints depends on stability and appropriate distribution of load across the joint surfaces, which in turn is dependent upon the geometry and material properties of the articulating joint tissue. Thus, the relationship of bone shape to OA development should be expected given that alterations in joint geometry affect joint congruity and can lead to maldistribution of load (48). Some bone shape changes may have adverse consequences for overlying cartilage. It has been hypothesized that cartilage loss is a mechanically mediated process that is more likely to occur in regions subjected to high stress, and such areas of high stress are likely to be influenced by bone shape (25).

While we demonstrated in this study that changes in bone shape precede the onset of radiographic OA by at least a year and longer, the latter event may be late in disease development. It is not clear how long some evidence of disease is present before it is apparent on the radiograph. However, two findings from our study may suggest that bone shape changes very early in the disease process, or perhaps may even be an inherent trait. First, knees with grade 0 radiographs and abnormal bone shapes were highly likely to develop OA. Second, bone shape even 2–4 years before radiographic OA incidence denoted an increased risk of disease (i.e., baseline bone shape irrespective of timing of later OA incidence). It is also possible that bone shape is an inherited factor that influences disease development and then changes further with the disease process. Addi-

tional longitudinal studies are needed to determine the ultimate relationship of bone shape to disease.

Much of the 3-D bone shape identified within this study is unlikely to be accurately or well-visualized on standard planar radiographs, particularly due to issues with projection, rotation, and resolution. A good example of this is that the growth of a distinctive ridge around the femoral plate appears in a radiograph as a small bony spur, and seems almost inconsequential. Changes in the bone such as flattening, widening, and ridge formation are difficult to quantify in radiograph studies, and are therefore not typically studied.

In addition to having analytic advantages as an imaging biomarker, many of these bone changes have implications for understanding OA pathophysiology and where the biomechanical stresses may be acting. For example, the widening and flattening of the bone structures is certain to change the distribution of mechanical load on the joint, presumably creating further change in bone. It also becomes apparent that alignment as well as the "joint space," which is thought to comprise cartilage and meniscus, are also influenced by bone shape. As OA progresses, some articular areas have bone laid down, while others appear to have bone "taken away." Osteophytes, which are generally described as discrete lesions on radiographs and morphologic assessments of MRI, can be seen to actually be a ridge-like laying down of bone circumferentially around the entire articular surface. This ridge may cause mechanical damage to other structures, such as the meniscus and overlying cartilage.

Previous studies that have examined the relationship of 2-D shape to OA (8,9,13) faced limitations of using manual markup from anteroposterior radiographs, including the inability to discern projection effects or rotation from true shape differences, and the inability to capture most of the 3-D shape changes (e.g., the patellofemoral joint and the osteophytic ridge). These are particularly difficult challenges for knee radiographs. An advantage to using MRI over radiographs to examine bone shape is obviously the 3-D nature of the data. MRIs also avoid difficulties in interpreting findings that may be related to positioning during image acquisition and to projection effects.

One prior small cross-sectional study used MRI to assess differences in the principal components of the tibia and femur geometry between the control and disease groups selected from the OAI using statistical shape modeling (17). However, in that study and other prior approaches, an independent test set was not used to validate the findings, which is necessary since it is highly likely when training a shape model that some

principal components will spuriously correlate with any labeling of the examples in the model (e.g., OA versus non-OA). In our study, we used independent training sets at each stage, thereby reducing the possibility of false-positive associations.

Another difference is our approach to analyzing the principal components derived from statistical modeling. Prior applications based on radiographs have analyzed individual principal components (or modes) to identify which one is the most discriminant (8,9,13,17), meaning that the data from the remaining principal components are not used. Our approach using LDA to identify a single vector takes into account information from all of the principal components that account for 98% of the variation, providing greater insight into correlated shape changes.

While our findings certainly point to the promise of such imaging and statistical methods for the prediction of knee OA onset and changes, certain limitations should be acknowledged. First, our methods required the assumption that shape change is linear. The model demonstrates that at least part of the change in OA is linear and systematic, although there may be other important effects which are nonlinear, or which occur only in subsets of individuals. Nonlinear approaches may be even more discriminating. Second, we modeled the shape change of whole bones, but local regional changes may be more sensitive and provide greater insight; this will be incorporated into future work. Third, a number of factors are likely to contribute to bone shape changes, including sex, race, BMI, alignment, and mechanical damage to the ligaments. Nonetheless, OA-related shape changes could be identified despite other contributors to change in shape. Fourth, early changes may not be the same as late changes, and therefore study of the full spectrum of OA development and progression is necessary.

In summary, we have demonstrated that MRI-based 3-D bone shape is associated with the development of incident radiographic knee OA, including that occurring 1 year later and beyond. The patterns of change provide opportunities to gain further insight into biomechanical and other pathophysiologic influences in OA pathogenesis. Use of AAM to comprehensively quantify MRI-based 3-D bone shape of the knee joint has potential as an imaging biomarker and warrants further study as an imaging end point in clinical trials.

AUTHOR CONTRIBUTIONS

All authors were involved in drafting the article or revising it critically for important intellectual content, and all authors approved the final version to be published. Dr. Neogi had full access to all of the data in the study and takes responsibility for the integrity of the data and the accuracy of the data analysis.

Study conception and design. Neogi, Bowes, Zhang, Felson.
Acquisition of data. Neogi, Bowes, De Souza, Vincent, Goggins, Felson.
Analysis and interpretation of data. Neogi, Bowes, Niu, De Souza, Vincent, Goggins, Zhang, Felson.

ROLE OF THE STUDY SPONSORS

Merck Research Laboratories, Novartis Pharmaceuticals Corporation, GlaxoSmithKline, and Pfizer, Inc. had no role in the study design, data collection, data analysis, data interpretation, writing of the manuscript, agreement to submit the manuscript for publication, or approval of the content of the submitted manuscript. Publication of the manuscript was not contingent upon the approval of Merck Research Laboratories, Novartis Pharmaceuticals Corporation, GlaxoSmithKline, or Pfizer, Inc.

ADDITIONAL DISCLOSURES

Authors Bowes, De Souza, and Vincent are employees of Imorphics Ltd.

REFERENCES

1. Guccione AA, Felson DT, Anderson JJ, Anthony JM, Zhang Y, Wilson PW, et al. The effects of specific medical conditions on the functional limitations of elders in the Framingham Study. Am J Public Health 1994;84:351–8.
2. Nguyen US, Zhang Y, Zhu Y, Niu J, Zhang B, Felson DT. Increasing prevalence of knee pain and symptomatic knee osteoarthritis: survey and cohort data. Ann Intern Med 2011;155:725–32.
3. Bingham CO III, Buckland-Wright JC, Garnero P, Cohen SB, Dougados M, Adami S, et al. Risedronate decreases biochemical markers of cartilage degradation but does not decrease symptoms or slow radiographic progression in patients with medial compartment osteoarthritis of the knee: results of the two-year multinational Knee Osteoarthritis Structural Arthritis study. Arthritis Rheum 2006;54:3494–507.
4. Hellio le Graverand-Gastineau MP, Clemmer R, Redifer P, Brunell RM, Hayes CW, Brandt K, et al. A 2-year randomized, double-blind, placebo-controlled, multicenter study of an oral selective iNOS inhibitor in subjects with symptomatic osteoarthritis of the knee [abstract]. Osteoarthritis Cartilage 2012;20 Suppl 1:S38.
5. Felson DT, Lawrence RC, Dieppe PA, Hirsch R, Helmick CG, Jordan JM, et al. Osteoarthritis: new insights. Part 1: the disease and its risk factors. Ann Intern Med 2000;133:635–46.
6. Goldring SR. The role of bone in osteoarthritis pathogenesis. Rheum Dis Clin North Am 2008;34:561–71.
7. Chen JH, Liu C, You L, Simmons CA. Boning up on Wolff's Law: mechanical regulation of the cells that make and maintain bone. J Biomech 2010;43:108–18.
8. Gregory JS, Waarsing JH, Day J, Pols HA, Reijman M, Weinans H, et al. Early identification of radiographic osteoarthritis of the hip using an active shape model to quantify changes in bone morphometric features: can hip shape tell us anything about the progression of osteoarthritis? Arthritis Rheum 2007;56:3634–43.
9. Lynch JA, Parimi N, Chaganti RK, Nevitt MC, Lane NE. The association of proximal femoral shape and incident radiographic hip OA in elderly women. Osteoarthritis Cartilage 2009;17:1313–8.
10. Baker-LePain JC, Lane NE. Relationship between joint shape and the development of osteoarthritis. Curr Opin Rheumatol 2010;22:538–43.

11. Dudda M, Kim YJ, Zhang Y, Nevitt MC, Xu L, Niu J, et al. Morphologic differences between the hips of Chinese women and white women: could they account for the ethnic difference in the prevalence of hip osteoarthritis? Arthritis Rheum 2011;63:2992–9.

12. Mahfouz M, Abdel Fatah EE, Bowers LS, Scuderi G. Three-dimensional morphology of the knee reveals ethnic differences. Clin Orthop Relat Res 2012;4701:172–85.

13. Haverkamp DJ, Schiphof D, Bierma-Zeinstra SM, Weinans H, Waarsing JH. Variation in joint shape of osteoarthritic knees. Arthritis Rheum 2011;63:3401–7.

14. Ding C, Cicuttini F, Scott F, Cooley H, Boon C, Jones G. Natural history of knee cartilage defects and factors affecting change. Arch Intern Med 2006;166:651–8.

15. Dore D, Quinn S, Ding C, Winzenberg T, Cicuttini F, Jones G. Subchondral bone and cartilage damage: a prospective study in older adults. Arthritis Rheum 2010;62:1967–73.

16. Reichenbach S, Guermazi A, Niu J, Neogi T, Hunter DJ, Roemer FW, et al. Prevalence of bone attrition on knee radiographs and MRI in a community-based cohort. Osteoarthritis Cartilage 2008; 16:1005–10.

17. Bredbenner TL, Eliason TD, Potter RS, Mason RL, Havill LM, Nicolella DP. Statistical shape modeling describes variation in tibia and femur surface geometry between Control and Incidence groups from the Osteoarthritis Initiative database. J Biomech 2010;43:1780–6.

18. Lester G. Clinical research in OA—the NIH Osteoarthritis Initiative. J Musculoskelet Neuronal Interact 2008;8:313–4.

19. Peterfy C, Li J, Zaim S, Duryea J, Lynch J, Miaux Y, et al. Comparison of fixed-flexion positioning with fluoroscopic semi-flexed positioning for quantifying radiographic joint-space width in the knee: test-retest reproducibility. Skeletal Radiol 2003;32: 128–32.

20. Felson DT, Nevitt MC, Yang M, Clancy M, Niu J, Torner JC, et al. A new approach yields high rates of radiographic progression in knee osteoarthritis. J Rheumatol 2008;35:2047–54.

21. Felson DT, Niu J, Guermazi A, Sack B, Aliabadi P. Defining radiographic incidence and progression of knee osteoarthritis: suggested modifications of the Kellgren and Lawrence scale. Ann Rheum Dis 2011;70:1884–6.

22. Cootes TF, Edwards GJ, Taylor CJ. Active appearance models. IEEE Trans Pattern Anal Mach Intell 2001;23:681–5.

23. Williams TG, Holmes AP, Bowes M, Vincent G, Hutchinson CE, Waterton JC, et al. Measurement and visualisation of focal cartilage thickness change by MRI in a study of knee osteoarthritis using a novel image analysis tool. Br J Radiol 2010;83:940–8.

24. Solloway S, Hutchinson CE, Waterton JC, Taylor CJ. The use of active shape models for making thickness measurements of articular cartilage from MR images. Magn Reson Med 1997;37:943–52.

25. Williams TG, Vincent G, Bowes M, Cootes T, Balamoody S, Hutchinson C, et al. Automatic segmentation of bones and inter-image anatomical correspondence by volumetric statistical modeling of knee MRI. Proceedings of the 2010 7th IEEE International Conference on Biomedical Imaging: from nano to macro; 2010 April 14–17; Rotterdam, The Netherlands. New York: Institute of Electrical and Electronic Engineers; 2010. p. 432–5.

26. Eckstein F, Hudelmaier M, Wirth W, Kiefer B, Jackson R, Yu J, et al. Double echo steady state magnetic resonance imaging of knee articular cartilage at 3 Tesla: a pilot study for the Osteoarthritis Initiative. Ann Rheum Dis 2006;65:433–41.

27. Hunter DJ, Bowes MA, Eaton CB, Holmes AP, Mann H, Kwoh CK, et al. Can cartilage loss be detected in knee osteoarthritis (OA) patients with 3–6 months' observation using advanced image analysis of 3T MRI? Osteoarthritis Cartilage 2010;18:677–83.

28. Cootes TF, Cooper D, Taylor CJ, Graham J. Active shape models—their training and application. Comput Vis Image Understanding 1995;61:38–59.

29. Cootes TF, Twining CJ, Petrovic V, Shchestowitz R, Taylor CJ. Groupwise construction of appearance models using piece-wise affine deformations. In: Clocksin WF, Fitzgibbon AW, Torr PH, editors. Proceedings of the British Machine Vision Conference; 2005 Sep 5–8; Oxford, UK. Oxford: BMVA Press; 2005. p. 88.1–88.10.

30. Fisher FA. The use of multiple measurements in taxonomic problems. Ann Eugenics 1936;7:179–88.

31. Davies RH, Twining CJ, Allen PD, Cootes TF, Taylor CJ. Shape discrimination in the hippocampus using an MDL model. Inf Process Med Imaging 2003;18:38–50.

32. Martinez AM, Kak AC. PCA versus LDA. IEEE Trans Pattern Anal Mach Intell 2001;23:228–33.

33. Sammon JW Jr. A nonlinear mapping for data structure analysis. IEEE Trans Comput 1969;C-18:401–9.

34. Bowes MA, DeSouza KM, Neogi T, Felson DT. Bone shape is not abnormal prior to OA but changes rapidly with OA development and may be a useful marker of OA occurrence. Osteoarthritis Cartilage 2010;18 Suppl 2:S19.

35. Buckland-Wright C. Subchondral bone changes in hand and knee osteoarthritis detected by radiography. Osteoarthritis Cartilage 2004;12 Suppl A:S10–9.

36. Radin EL, Rose RM. Role of subchondral bone in the initiation and progression of cartilage damage. Clin Orthop Relat Res 1986;213:34–40.

37. Grynpas MD, Alpert B, Katz I, Lieberman I, Pritzker KP. Subchondral bone in osteoarthritis. Calcif Tissue Int 1991;49:20–6.

38. Li B, Aspden RM. Mechanical and material properties of the subchondral bone plate from the femoral head of patients with osteoarthritis or osteoporosis. Ann Rheum Dis 1997;56:247–54.

39. Li B, Aspden RM. Composition and mechanical properties of cancellous bone from the femoral head of patients with osteoporosis or osteoarthritis. J Bone Miner Res 1997;12:641–51.

40. Patel V, Issever AS, Burghardt A, Laib A, Ries M, Majumdar S. MicroCT evaluation of normal and osteoarthritic bone structure in human knee specimens. J Orthop Res 2003;21:6–13.

41. Messent EA, Buckland-Wright JC, Blake GM. Fractal analysis of trabecular bone in knee osteoarthritis (OA) is a more sensitive marker of disease status than bone mineral density (BMD). Calcif Tissue Int 2005;76:419–25.

42. Woloszynski T, Podsiadlo P, Stachowiak GW, Kurzynski M, Lohmander LS, Englund M. Prediction of progression of radiographic knee osteoarthritis using tibial trabecular bone texture. Arthritis Rheum 2012;64:688–95.

43. Kraus VB, Feng S, Wang S, White S, Ainslie M, Brett A, et al. Trabecular morphometry by fractal signature analysis is a novel marker of osteoarthritis progression. Arthritis Rheum 2009;60: 3711–22.

44. Dieppe P, Cushnaghan J, Young P, Kirwan J. Prediction of the progression of joint space narrowing in osteoarthritis of the knee by bone scintigraphy. Ann Rheum Dis 1993;52:557–63.

45. Day JS, Ding M, van der Linden JC, Hvid I, Sumner DR, Weinans H. A decreased subchondral trabecular bone tissue elastic modulus is associated with pre-arthritic cartilage damage. J Orthop Res 2001;19:914–8.

46. Shepstone L, Rogers J, Kirwan JR, Silverman BW. Shape of the intercondylar notch of the human femur: a comparison of osteoarthritic and non-osteoarthritic bones from a skeletal sample. Ann Rheum Dis 2001;60:968–73.

47. Wada M, Tatsuo H, Baba H, Asamoto K, Nojyo Y. Femoral intercondylar notch measurements in osteoarthritic knees. Rheumatology (Oxford) 1999;38:554–8.

48. Bullough PG. The geometry of diarthrodial joints, its physiologic maintenance, and the possible significance of age-related changes in geometry-to-load distribution and the development of osteoarthritis. Clin Orthop Relat Res 1981;156:61–6.